FUSION EVENTS AND NONFUSION CONTENTS MIXING EVENTS INDUCED IN ERYTHROCYTE GHOSTS BY AN ELECTRIC PULSE

ARTHUR E. SOWERS
Holland Laboratory, American Red Cross, Rockville, Maryland 20855

ABSTRACT The mechanism of membrane fusion was studied by using human erythrocyte ghosts held in close contact by alternating current-induced dielectrophoresis and inducing fusion with a single electric field pulse. Individual fusion events were followed visually using either 1,1'-dihexadecyl-3,3,3',3'-tetramethylindo carbocyanine perchlorate as a membrane-mixing label or 10-kD fluorescein isothiocyanate–dextran as a contents-mixing label. However, over a range of variables, the number of contents-mixing events usually considerably exceeded the number of membrane-mixing events, although the discrepancy was less at higher ionic strength. However, when the dielectrophoretic force holding the membranes in contact was turned off after the pulse, Brownian motion caused some of the groups of ghosts in which contents mixing occurred to eventually separate from one another, showing that they could not represent fusion events. Separate experiments showed, conversely, that fusion did occur in the groups that did not separate after the dielectrophoresis was turned off.

INTRODUCTION

Membrane fusion is an essential step in many biological processes, but its molecular mechanism is poorly understood. Studies of membrane fusion have previously utilized a variety of membrane systems and induced fusion with, for example, chemicals, proteins, lipid composition manipulation, laser pulses, or strong direct current electric field (EF) pulses (1–11, for reviews). For this paper, EF pulses were used to study fusion induced in human erythrocyte ghosts to both elucidate the fusion mechanism and to ascertain what aspects of the mechanism may be relevant to naturally occurring fusion. Although close membrane–membrane contact—required for fusion in any system—can be induced in many ways, alternating current (AC)-induced dielectrophoresis (12) was used in this study to induce membrane–membrane contact because it is a mild, completely reversible, and nonchemical effect.

Use of an EF pulse to induce fusion (electrofusion) was significant because the current from the pulse could be present for <1–2 ms, was nonchemical, and could induce high fusion yields. High fusion yields made it practical to study single fusion events. The use of electrofusion to study fusion mechanisms is interesting because there is evidence that there may be two different mechanisms (8, 13–15).

The research reported here (*a*) suggests a basis for an apparent discrepancy between two fusion assays, (*b*) resolves conflicting reports pertaining to a permeabilization effect, which could affect the results of one of the fusion assays, and (*c*) suggests the possibility that electrofusion may proceed through the reversible induction of a distinct intermediate stage. Portions of this paper were reported in preliminary form (16).

METHODS

Membrane Preparation

Ghost membranes were isolated from packed human erythrocytes and washed in pH 7.4 isotonic sodium phosphate buffer. Hemolysis and washes were done, respectively, in 5 and 20 mM sodium phosphate buffer (pH 8.5) and labeled in the cytoplasmic compartment with 10-kD fluorescein isothiocyanate–dextran (FD) through the hemolytic hole (17) and membrane-labeled with 1,1'-dihexadecyl-3,3,3',3'-tetramethylindo carbocyanine perchlorate (DiI), as previously described (14, 18). Ghosts were stored in the 20 mM buffer overnight. The next day the ghosts were used at a buffer strength of 20 mM or pelleted and resuspended with a buffer strength of 60 mM (pH 8.5) to study the effect of a change in ionic strength. The fusion assays were conducted at 20–22°C, all other operations were conducted at 0–4°C.

Apparatus

The chamber in which dielectrophoresis and fusion were induced and observed by light microscopy was previously described (18). Electric pulses with an exponentially decaying waveform were generated by using a type 5557 mercury vapor thyratron to discharge a capacitor through the membrane suspension medium; the circuit diagram and other details are described elsewhere (19). Pulse parameters (voltage and decay halftime) were continuously monitored using a Tektronix Inc. (Beaverton, OR) model T912 storage oscilloscope. Pulse field strength in the chamber was determined by dividing the pulse voltage applied at the electrodes by the chamber length (2 mm), as previously described (18). Light microscopy was done with a Zeiss model 14 microscope equipped for phase contrast and epifluorescence. Micrographs were made by single frame playback on a Panasonic model NV-9300A videocassette recorder of videotaped sequences obtained with a Zeiss three-stage low light level Venus

Camera. Date and time alphanumerics were generated with a FOR-A (West Newton, MA) model VTG-22 video timer.

Normal Fusion Protocol

The ratio of labeled (either membrane-labeled or containing FD) to unlabeled ghosts in the chamber was 1:15. Close membrane–membrane contact was induced by aligning the ghosts into pearl chains using dielectrophoresis (12). The field strength of the dielectrophoresis-inducing alternating current (60 Hz) in the chamber was 10–13 V/mm. After alignment, fusion was induced with a single DC pulse (field strength, 500–700 V/mm; decay halftime, 0.6–1.0 ms). Contents-mixing events and membrane-mixing events were enumerated by first aligning the ghosts into pearl chains (taking ~10–15 s) and then passing a single DC pulse through the suspension. However, the alternating current was present in the suspension after as well as before the pulse and thus continued to hold all membranes in contact regardless of whether they fused.

Protocol Modifications

In some experiments the AC was turned off immediately after the pulse to determine which membranes became attached to each other as a result of fusion and which membranes separated, thereby revealing that they did not become fused. Separation of a given pair of membranes could be determined as soon as 2 s but, in some cases, required up to 2 min of continuous observation.

Fusion Yield Calculation

Percent fusion yield (FY) was calculated by counting in a field of view the total number of events, N_f, in which the pulse caused the fluorescence to move from an originally labeled membrane to at least one originally unlabeled membrane in the same pearl chain and also counting, N_u, the total number of originally labeled membranes in which the label did not move to an adjacent unlabeled membrane. Fusion yield was calculated as $FY = N_f/(N_f + N_u) \times 100$. To avoid counting false membrane-mixing events due to happenstance alignment of two labeled ghosts into adjacent positions, counts were started only when gradients of laterally diffusing DiI became visible (10–15 s after the pulse) but completed before lateral equilibration in fluorescence was achieved (~1 min after the pulse). Likewise, to avoid counting false contents-mixing events, a sample field was examined by focusing up and down through the volume of the chamber before the pulse to determine if doublets were present. Sample size was always $80 < (N_f + N_u) < 120$.

Determining Whether Pulse-induced Electropores Are in One or Two Hemispheres of Ghosts

Testing the hypothesis that electropores are induced in both hemispheres of a spherocytic ghost required an experiment to overcome any electrokinetic factors that would cause only unidirectional movement toward the negative electrode (see below). This was done by causing the release of FD from a FD-containing ghost into a transient cloud just over the positive-facing hemisphere of the ghost that did not contain FD. To aid in recording the position of both the ghost not containing FD and the FD-containing ghost, all of the former were labeled faintly with DiI while the later were loaded to the point of saturating the video level. Also, the two membranes had to be positioned (*a*) 1–3-μm apart, (*b*) on an axis in the focal plane parallel to the pulse field direction, and (*c*) the ghost not containing FD had to be closer to the negative electrode. This was done by including pearl chains and then turning off the AC for a short while just before the pulse was applied in order to allow the ghosts to separate a short distance by Brownian motion. All sequences were videotaped by the low light level camera but pulses were applied only when the proper separation was achieved.

Relationship between Pulse-induced (*a*) Attachment, (*b*) Contents Mixing, (*c*) Membrane Mixing, and (*d*) Fusion

A pulse was applied to dielectrophoretically aligned mixtures of DiI-labeled or FD-containing ghosts and unlabeled ghosts (ratio of 1:15). After the pulse, the AC was immediately turned off. Viewing by phase and fluorescence optics was continuously alternated while selecting only those ghosts that became attached to each other by the pulse treatment and had at least one fluorescent ghost present. Members of this subset of ghosts were divided into one of two categories: (*a*) fluorescence in only one ghost, or (*b*) fluorescence in two or more adjacent ghosts. In the case of DiI, the fluorescence in the attached groups was counted as being in two or more ghosts only if gradients were seen. In the case of FD, the fluorescence in pulse-induced attached groups was also scored as either in one or two or more adjacent ghosts but the sample volume was viewed before the pulse to detect happenstance adjacent alignment of FD-labeled ghosts before the pulse was applied.

RESULTS

Relationships between Event Indicators and Fusion

Nearly all (>99%) of the ghosts in pearl chains which became attached to each other as a result of the pulse (700 V/mm, 0.6-ms decay halftime) and which had at least one DiI-labeled membrane also showed gradients of DiI diffusing into originally unlabeled membranes in mixtures of unlabeled and labeled ghosts. Therefore, a pulse-induced attachment event represents a fusion event. Fluorescence was almost always ($N = 198$) found in two or more adjacent ghosts but almost never ($N = 2$) in only one member after the pulse in those ghosts that became attached to each other to form a group and had just one FD-containing membrane present before the pulse. Therefore, an attachment event almost never occurs without contents mixing taking place. However, a contents-mixing event can occur without attachment (see below).

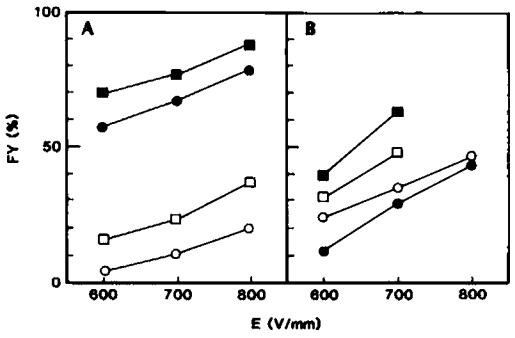

FIGURE 1 Fusion yields induced by a single EF pulse of strength E (V/mm) in erythrocyte ghosts that were previously aligned and held in close contact by dielectrophoresis both before, during, and after the pulse. Medium is sodium phosphate buffer (pH 8.5) of strength (*A*) 20 mM or (*B*) 60 mM. Data points are: FD (*solid symbols*); DiI (*open symbols*). Pulse decay halftime in *A* is 0.6 ms (*circles*), 1.0 ms (*squares*); and in *B* is 0.6 ms (*circles*); 0.8 ms (*squares*).

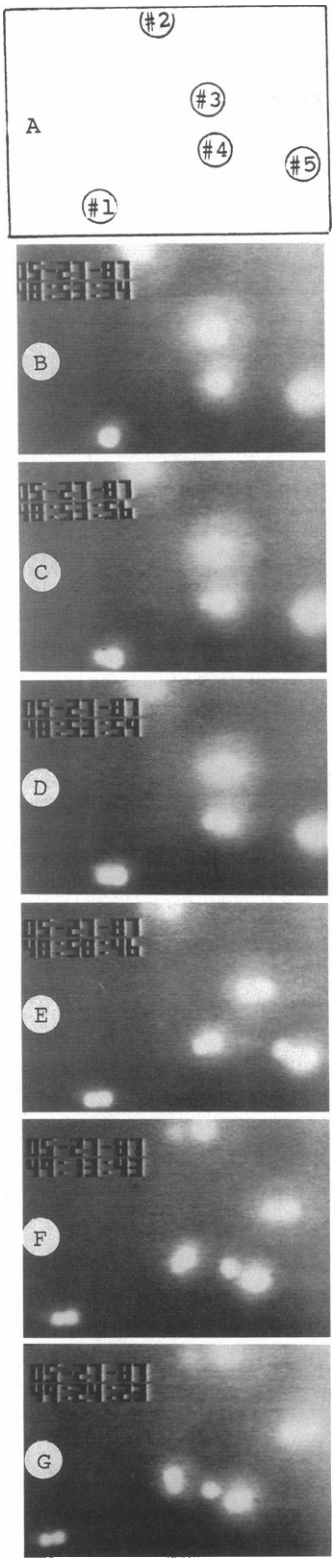

FIGURE 2 Low light level video sequence of fluorescence movements in mixtures of unlabeled (not visible) and five FD-labeled (*white circles*) ghosts aligned by dielectrophoresis into pearl chains in 20 mM sodium phosphate (pH 8.5), and treated with a single pulse (600 V/mm, 0.6 ms decay halftime). The axes of all aligned pearl chains were parallel to one another and oriented left-right. The axis of the field pulse (600 V/mm, 0.8-ms decay haltime) is left-right with the negative electrode at left. Immediately after the pulse the AC was turned off to allow Brownian motion to reveal which contents-mixing events were accompanied by irreversible attachment. Alphanumerics: (*upper*) month-day-year; (*lower*) min:s:1/100 s. Pulse is applied at 48:53:56. (*A*) Labeled membranes are numbered 1–5 for reference purposes. (*B–G*) Note that fluorescence moves toward negative electrode (*left*) for all ghosts in field of view. Movement of fluorescence is complete by 48:53:59 (30 ms after the pulse). Images of ghosts *3*, and to a lesser extent *2* and *4*, are obscured (*a*) by a localized leakage of fluorescence to the background which is simultaneous with the pulse; (*b*) by image blur due to position out of the focal plane; and (*c*) because the video system gain was set slightly above saturation to capture subequilibrium amounts of fluorescence, which became trapped in the unlabeled ghost adjacent to the FD-labeled ghost (e.g., unlabeled ghost receiving fluorescence from labeled ghost *2* as seen in *F*). Note that 20 s after AC was turned off, separation (indicating unfused membranes) clearly occurs for ghost doublets *2* and *5*, but not for doublet *1*. Status of doublets *3* and *4* is obscured by significant Brownian motion-induced tumbling. Note that fluorescence loss in *1*, due to small but long-lived pulse-induced permeability increase occasionally seen in some ghosts, caused the diameter of the ghost image to diminish with time. Photo width, 100 μm.

Fusion Yields with Normal Protocol (AC On before and after the Pulse)

Each measurement of FY based on the use of either FD or DiI was experimentally reproducible to 2–3% for ghosts from a single blood donor, but different donors showed a variability which showed up as lines shifted higher or lower in position but parallel to each other. An increase in pulse field strength or pulse decay halftime caused an increase in fusion yield (Fig. 1). However, when both labels were used in separate but identical experiments using the same ghost preparation, FD-based FYs were nearly always much higher than DiI-based FYs (the exception is the data for 60 mM and $T_{1/2}$ = 0.6 ms). Equally important, an increase in buffer (ionic) strength reduced the magnitude of the discrepancy: the DiI-based FY increased somewhat while the FD-based FY decreased markedly.

Effect of Turning the AC Off after Pulse

When FD was the fusion indicator and the AC was turned off immediately after the pulse, then some of the groups of two or three contiguously labeled ghosts stayed attached to each other. The others eventually drifted apart due to Brownian motion while retaining the same level of fluorescence (Fig. 2). An increase in buffer strength from 20 to 60 mM caused an increase in the fraction of all contents-mixing events in which the ghosts became attached as a result of the pulse treatment (Fig. 3).

Preferential Movement of Contents-mixing Indicator (Fig. 2)

Over a wide range of pulse field strengths (500–800 V/mm) and decay halftimes (0.6–1.2 ms), the movement of FD into unlabeled ghosts flanking the FD-containing ghosts was preferentially greater (66–96%) toward the negative electrode in all samples of assayed ghosts in a chamber. In the remainder of the contents-mixing events

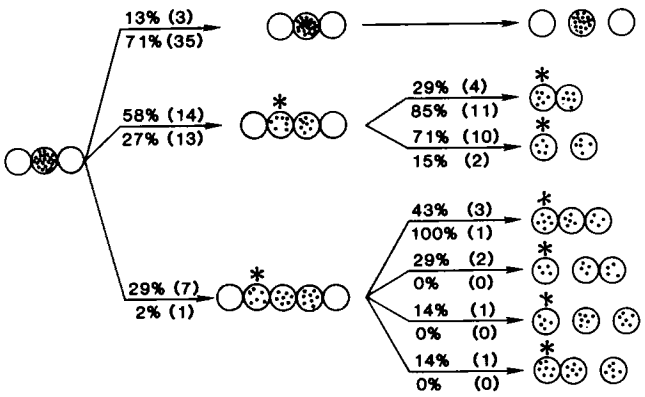

FIGURE 3 Post-pulse fate of aligned ghosts in which contents-mixing events took place and were observed continuously by both phase and fluorescence optics for up to 2–3 min after the AC was turned off. Pulse characteristics: 600 V/mm, 0.6-ms decay halftime. Numbers reflect only contents-mixing events in which FD moved only toward negative electrode from an originally labeled membrane (*). (*Left*) Prepulse view (AC = on). (*Middle*) Post-pulse view (AC = on). (*Right*) Post-pulse view 2–3 min after AC was turned off. Notes: Although separated membranes on right are drawn on a pearl chain axis, the membranes actually separated from one another in random directions (cf. Fig. 2); only one unlabeled ghost is shown on each side of 1–3 contiguously labeled ghosts even though pearl chains contain 10–30 ghost members. Percent numbers refer to relative frequency of occurrence along that pathway and were calculated from contents-mixing events (*lower two paths*) or no contents mixing (*upper path*) and are not, per se, related to fusion yield as used elsewhere in this paper. Numbers in parentheses refer to actual numbers of contents-mixing events counted and used in the calculation. Buffer strengths: above arrows, 20 mM; below arrows, 60 mM.

(34–4%), the pulse-induced movement of FD occurred about equally either towards the positive electrode or in both directions from a labeled membrane.

Both Hemispheres of a Spherical Membrane Become Permeabilized by a Pulse (Fig. 4)

Ghosts not containing FD (not fluorescent) became partially fluorescent after a transient cloud of FD was released over their positive electrode-facing hemispheres (Fig. 4). This occurred as a cloud of fluorescence originating from the FD-containing ghosts appeared in the space between the FD-containing ghost and the ghost not containing FD. The fluorescence intensity and size of the cloud peaked by 0.12 s after the pulse and then faded into the background by 0.2–0.3 s after the pulse. By the time the cloud faded into the background, the ghost originally not containing FD showed a significant increase in fluorescence.

Lifetime of Contents-mixing Event

Movement of the fluorescence from FD-containing ghosts to ghosts not containing FD in a pearl chain during a contents-mixing event either ends with an equal amount of fluorescence in all labeled ghosts or with more fluorescence remaining in the originally labeled ghost. The contents-mixing events ended as soon as ~30 ms (Fig. 2) or as late as 200 ms after the pulse (not shown). However, regardless of whether separation occurred when the AC was turned off after the pulse, there is little or no subsequent decrease in the level of fluorescence in the ghosts other than bleaching (Fig. 2).

DISCUSSION

Criteria for Fusion

The first morphological change which demonstrates fusion in two spherical membranes in contact is the appearance of the hour-glass shape. A continuous increase in the diameter of the hour-glass constriction (lumen) eventually leads to a single large sphere. However, a previous study revealed that fusion of human erythrocyte ghosts leads to both lumen-producing fusion products and nonlumen-producing fusion products (18). The nonlumen-producing ghost fusion products were not detectable by using phase optics because the lumen diameter never increased enough to be distinct. They were detected, on the other hand, by observing time-dependent lateral diffusion of DiI to an adjacent unlabeled membrane in a pearl chain.

Rigorous criteria for membrane fusion include a requirement for (*a*) connection of the originally separate membranes to permit any membrane component to have access to all membrane area by lateral diffusion (membrane mixing), and (*b*) connection of the originally separate enclosed spaces (contents mixing) (references 2, 9, 20–22). From these criteria it would be expected that every fusion event should be accompanied by both a contents-mixing event and a membrane-mixing event. Therefore, the use of membrane or soluble labels to indicate both categories of event in separate but identical experiments should lead to identical fusion yields. However, in our experiments the contents-mixing events usually exceeded membrane-mixing events by a considerable margin (Fig. 1).

When the AC was turned off after the pulse in the contents-mixing experiments (Fig. 3), it showed that an appreciable number of contents-mixing events actually did not represent fusion. This is significant because it reveals the origin of the discrepancy. Because the results in Fig. 3 were from ghosts obtained from a different blood donor than for the results in Fig. 1, it would not have been valid to derive a "corrected" contents-mixing fusion yield by subtracting the number of nonfusion events from the total number of events. However, the results in Fig. 3 did show that an increase in the ionic strength of the medium caused a large decrease in the proportion of nonfusion contents-mixing events and a concomitant but small increase in the proportion of fusion-related contents-mixing events. This is significant because it revealed (*a*) a factor (ionic strength) which determines the magnitude of the discrepancy, and (*b*) an increase in ionic strength increased fusion yield.

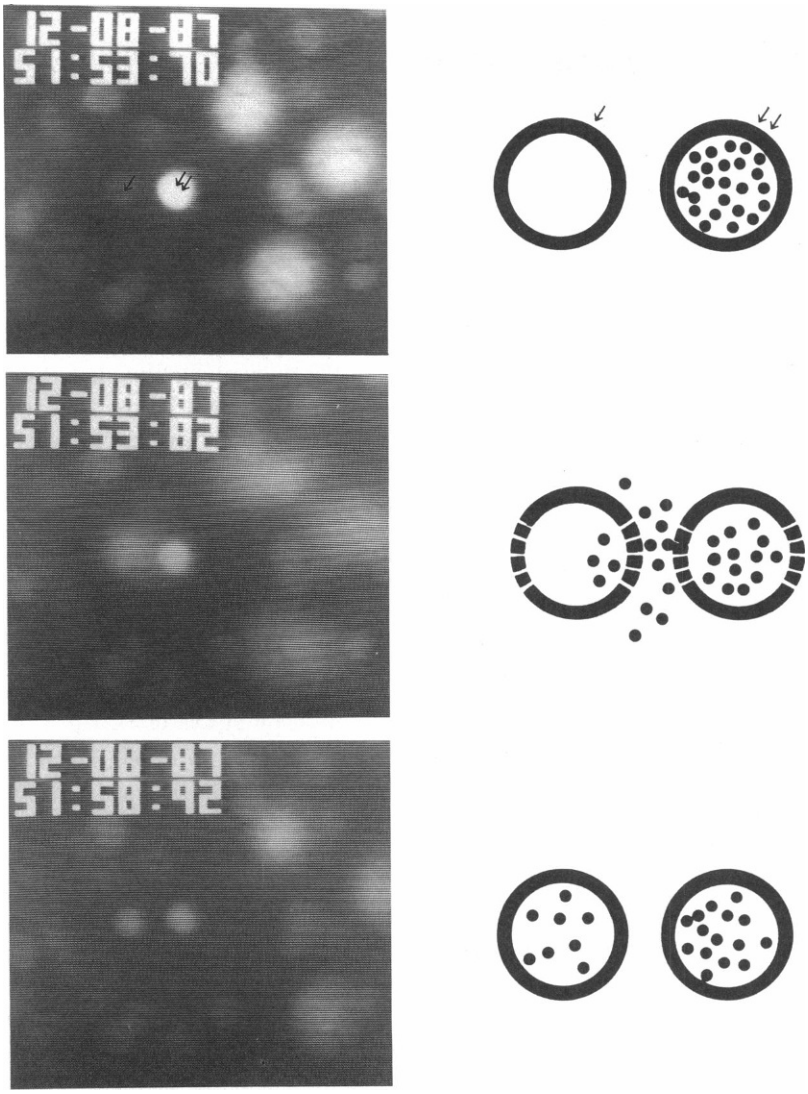

FIGURE 4 Evidence of electropore induction in both hemispheres of spherical-shaped erythrocyte ghosts. Accumulation of 10-kD FITC–dextran (FD) into a ghost not labeled with FD (*single arrow*) from a transient cloud of FD produced just over the positive electrode-facing hemisphere as produced through electropores in the negative electrode-facing hemisphere of a nearby FD-labeled ghost (*double arrow*). Ghosts not labeled with FD were faintly labeled with DiI to reveal positions. FD-labeled ghost is located closer to the positive electrode (*right*) and on an axis with the electric field pulse (left-right, and in plane of focus). *Left*, micrographs of selected frames of video sequence; *right*, illustration of corresponding permeabilization state of respective ghosts (*circles*) and location of FD molecules (*dots*); *top*, pre-pulse view showing four (three are out of focal plane) brightly FD-labeled ghosts surrounded by the faintly DiI-labeled ghosts; *middle*, same ghosts 120 ms after a single EF pulse (700 V/mm, 0.8-ms decay halftime). Note appearance of diffuse cloud of fluorescence centered in space between two ghosts but extending a radius of ~4 μm in all directions. *Bottom*, same ghosts after most of fluorescence in cloud has diffused into background. Note (*a*) the increase in fluorescence from DiI-labeled ghosts and decrease in fluorescence from all FD-labeled ghosts; (*b*) no significant change in fluorescence of other, DiI-labeled ghosts.

Contents-Mixing Events without Fusion

Contents-mixing events that are not accompanied by attachment (i.e., fusion) could be due to (*a*) a return to the unfused membranes after fusion by a reversal of the fusion process, (*b*) an artifact, or (*c*) the reversible formation of a fusion-intermediate structure on the way to a fusion product. The first possibility is unlikely because both the fusion product and the close-spaced pair of unfused membranes should be low energy configurations compared with any high energy (unstable) intermediate structure. The second possibility may be due to membrane pores (electropores), which are known to be induced by the same pulses that induce membrane fusion (23–25). These pores could allow FD to leak out of a labeled ghost and then into adjacent unlabeled ghosts in a pearl chain and otherwise not be distinguishable from a fusion-related contents-mixing event. The third possibility would permit contents mixing to take place during the lifetime of the intermediate structure. This interval begins when contents mixing becomes detectable and ends when no further change in contents mixing is observed or actual membrane fusion becomes irreversible. However, the intermediate then goes out of existence by either going forward to a fusion product or back to unfused but close-spaced membranes.

The second possibility, namely that electropores cause the excess nonfusion contents-mixing events, must be considered within the framework of three relevant reports which indicate that the amount of pulse-induced permeabilization differs significantly in each of the two hemispheres facing each electrode (26–28). The reports also disagree as to which hemisphere has the greater degree of permeabilization. The possibility of a very low or zero permeability in either hemisphere would, therefore, work against the hypothesis that electropores could be responsible for the excess number of contents-mixing events.

In a previous study from this laboratory, the pulse-induced permeabilization always appeared to be in the negative electrode-facing hemisphere (26). In this study the FD moved preferentially toward the negative electrode

during contents-mixing events (e.g., Fig. 2). Therefore, the absence of movement through the positive-facing hemisphere must be due to either a subdetectable level of permeabilization or a factor that prevents efflux. The latter possibility was shown to be the case since fluorescence became trapped in a ghost from a transient cloud of FD released from one ghost just over the positive-electrode facing hemisphere of a second ghost during a pulse (Fig. 4). Thus, the fluorescence moved into the second ghost while the pores were open. After they closed, any fluorescence inside both ghosts was then trapped while the remaining fluorescence in the cloud outside the ghosts diffused to the background. This result showed that electropores were induced in both hemispheres, but all movement of fluorescence occurred only toward the negative electrode.

The unidirectional flow through electropores could be caused by electroosmosis (29). Electroosmosis occurs when an electric field parallel to a charged surface in contact with an ionic aqueous medium causes a net hydrodynamic flow toward the electrode with the polarity opposite to the dominant charge in the medium just near the surface. In the present case, the negative charge of the phospholipid headgroups at the edge of the pore attract a greater number of positive charges than negative charges. A net flow will thus occur toward the negative electrode with an electric field parallel to the axis of the pore or, in other words, perpendicular to the plane of the membrane. Indeed, this explanation resolves the disagreement about which hemisphere becomes more permeabilized. Thus, if a permeability tracer moves into the cells from the outside (as in references 27 and 28), then it can only go inward through the positive-facing hemisphere. Conversely, the outward movement of a tracer from the interior of an erythrocyte ghost (as in reference 26) can thus only be seen in the negative-facing hemisphere. Moreover, the fact that electroosmosis effects are diminished at higher ionic strengths is consistent with the diminished discrepancy observed between the contents-mixing events and the membrane-mixing events when the buffer strength is 60 mM instead of 20 mM.

The buildup phase in fluorescence from the pulse-induced transient cloud of FD was complete by 120 ms (see Results). At this instant in time the influx to the cloud from the FD-containing ghost must match outflux to the background. Assuming the fluorescence buildup as a roughly S-shaped curve, it can be estimated that the induced electropores must have started to close by ~60 ms and finished closing by 120 ms or soonor after the pulse. The exponential decay of the electric pulse waveform permits a significant field strength to exist for many decay halftimes after the voltage rises at the leading edge of the pulse. Furthermore, the capacitance of the membrane will permit a pulse-induced transmembrane voltage to persist for an even longer interval. Thus it is reasonable for flow to continue longer than the duration of the pulse. Major unknown factors needed to more accurately relate the extent of electroosmosis flow to the pulse duration include (*a*) the time dependence and magnitude of the electropore-based shunt resistance, which would control the discharge rate of the membrane, (*b*) the mechanism of electropore resealing, which may not have a simple relationship to membrane viscosity, and (*c*) the amount of transmembrane voltage needed to hold a pore open compared with the voltage needed to open a pore.

Thus, movement of FD through pores in adjacent hemispheres of the close-spaced ghosts in pearl chains is possible and could lead to some nonfusion contents-mixing events. However, the top pathway in Fig. 3 clearly shows that a pulse often fails to cause a contents-mixing event! Indeed in these cases the ghosts originally not containing FD which are adjacent to FD-containing ghosts in a pearl chain received absolutely no visually detectable fluorescence. This is unexpected since virtually all FD-labeled ghosts become substantially permeabilized by the same pulse when they are in random positions in suspension (26)! It is possible that the permeabilization response of the ghosts to the electric field pulse may be different when the ghosts are in pearl chains (i.e., in close contact) compared with random positions in suspension. This interpretation is at least partly supported by the observation of a small but significant number (4–34%) of contents-mixing events which occur by moving either in both directions or only toward the positive electrode. It is also possible that there is enough compositional difference between individual membranes to cause different responses. Hence, interpreting a nonfusion contents-mixing event as a fusion intermediate or as an effect of electroporation and electroosmosis cannot be decided by the present experiments.

If the nonfusion contents-mixing events do represent the reversible formation of fusion intermediate structures, then it is possible to estimate their lifetimes. The pulse caused contents mixing to be clearly observable within the interval of one videoframe (16.6 ms) and either come to equilibrium (same level of fluorescence in both originally labeled and originally unlabeled spaces) by the completion of the second videoframe ~33 ms later (Fig. 2). In other video sequences (not shown) the equilibration took as long as 200 ms. Single-frame playback of many video sequences suggested that there was no obvious relationship between lifetime and the question of whether two particular membranes also became attached (i.e., fused). The observation that the process of contents mixing was interrupted before equilibration in fluorescence levels was achieved can be interpreted in two ways depending on whether the ghosts in question also became attached or not. If they became attached, then the contents-mixing event reflects fusion and the diameter of the lumen must either contract to a diameter less than or equal to the molecular diameter of the FD. If they did not become attached, then the lumen did not pass the midpoint and stabilize, but, instead, reverted back to unfused membranes. For the cases where

both equilibration in fluorescence and attachment were achieved, then it was impossible to determine whether the lumen diameter was greater or less than the diameter of the probe.

It may also be significant that the contents-mixing lifetimes of 30–200 ms as reported here are consistent with the capacitance flicker lifetimes of up to 120–240 ms observed during granule secretion, which have also been interpreted to represent the reversible formation of fusion intermediate structures (30–32).

It can be concluded from this study that the descrepancy between the contents-mixing assay and the membrane-mixing assay was due to contents-mixing events that did not represent fusion. These nonfusion contents-mixing events can be identified, however, if the assay is modified to include a step in the protocol to test for fusion in addition to the contents-mixing events. While nonfusion contents-mixing events may be due to an artifactual contribution from electroosmosis during the lifetime of induced electropores, they may also indicate the presence of a reversibly inducible fusion intermediate structure. To the author's knowledge, the recognition of significant electroosmosis effects at the edge of electropores is the first report of its kind in the electropore literature (33). Also, ionic strength appears to play a significant fundamental role in the fusion mechanism since it leads to higher fusion yields regardless of whether the assay is based on membrane mixing or the dual criteria of contents mixing and attachment. If nonfusion contents-mixing events do represent fusion intermediates, then higher ionic strength favors fusion product formation over a return to unfused membranes. The finding that pulse-induced attachment between ghosts detects all nonlumen fusion products is significant for the design of future experiments because it is possible to use phase optics and the criterion of nonseparation after cessation of dielectrophoresis to detect fusion products independently of the presence of any fluorescent indicator. The present study also shows that it may be feasible to study single fusion–related contents-mixing events and membrane-mixing events simultaneously in the same two membranes by double labeling with suitable tracers.

This work was supported by ONR contract N00014-87-K-0199.

The technical assistance of Ms. Veena Kapoor is gratefully acknowledged.

Received for publication 8 December 1987 and in final form 10 June 1988.

REFERENCES

1. Bates, G. W., J. A. Saunders, and A. E., Sowers. 1987. Electrofusion principles and applications. *In* Cell Fusion. A. E. Sowers, editor. Plenum Press, New York. 367–395.
2. Blumenthal, R. 1987. Membrane fusion. *Cur. Top. Membr. Transp.* 29:203–254.
3. Dimitrov, D. S., and R. K. Jain. 1984. Membrane stability. *Biochim. Biophys. Acta.* 779:437–468.
4. Lucy, J. A. 1978. Mechanisms of chemically induced cell fusion. *In* Membrane Fusion. G. Poste and G. L. Nicolson, editors. Elsevier/North Holland, Amsterdam. 267–304.
5. Nir, S., J. Bentz, J. Wilschut, and N. Duzgunes. 1983. Aggregation and fusion of phospholipid vesicles. *Prog. Surf. Sci.* 688:1–124.
6. Rand, R. P., and V. A. Parsegian. 1986. Mimicry and mechanism in phospholipid models of membrane fusion. *Annu. Rev. Physiol.* 48:201–212.
7. Schierenberg, E. 1987. Laser-induced cell fusion. *In* Cell Fusion. A. E. Sowers, editor. Plenum Press, New York. 409–418.
8. Sowers, A. E., and V. Kapoor. 1987. The electrofusion mechanism in erythrocyte ghosts. *In* Cell Fusion. A. E. Sowers, editor. Plenum Press, New York. 397–408.
9. Szoka, F. C. 1987. Lipid vesicles: model systems to study membrane-membrane destabilization and fusion. *In* Cell Fusion. A. E. Sowers, editor. Plenum Press, New York. 209–240.
10. White, J., M. Kielian, and A. Helinius. 1983. Membrane fusion proteins of enveloped animal viruses. *Quart. Rev. Biophys.* 16:151–195.
11. Zimmermann, U. 1982. Electric field-mediated fusion and related electrical phenomena. *Biochim. Biophys. Acta.* 694:227–277.
12. Pohl, H. A. 1978. Dielectrophoresis. Cambridge University Press, Cambridge, UK. 579 pp.
13. Teissie, J., and M. P. Rols. 1986. Fusion of mammalian cells in culture is obtained by creating the contact between cells after their electropermeabilization. *Biochem. Biophys. Res. Commun.* 140:258–266.
14. Sowers, A. E. 1986. A long-lived fusogenic state is induced in erythrocyte ghosts by electric pulses. *J. Cell Biol.* 102:1358–1362.
15. Sowers, A. E. 1987. The long-lived fusogenic state induced in erythrocyte ghosts by electric pulses is not laterally mobile. *Biophys. J.* 52:1015–1021.
16. Sowers, A. E. 1987. Evidence for a fusion intermediate in electrofusion. *Biophys. J.* 53:325a. (Abstr.)
17. Lieber, M. R., and T. L. Steck. 1982. A description of the holes in human erythrocyte membrane ghosts. *J. Biol. Chem.* 297:11651–11659.
18. Sowers, A. E. 1984. Characterization of electric field-induced fusion in erythrocyte ghost membranes. *J. Cell Biol.* 99:1989–1996.
19. Sowers, A. E. 1988. The mechanism of electrically-induced fusion in erythrocyte membranes. *In* Electroporation and Electrofusion in Cell Biology. E. Neumann, A. E. Sowers, and C. Jordan, editors. Plenum Press, New York. In press.
20. Morris, S. J., D. Bradley, C. C. Gibson, P. D. Smith, and R. Blumenthal. 1988. Use of membrane-associated fluorescence probes to monitor fusion of bilayer vesicles: application to rapid kinetics using pyrene excimer/monomer fluorescence. *In* Spectroscopic Membrane Probes. L. M. Loew, editor. CRC Press, Boca Raton, FL. 161–191.
21. Duzgunes, N., and J. Bentz. 1988. Fluorescence assays for membrane fusion. *In* Spectroscopic Membrane Probes. L. M. Loew, editor. CRC Press, Boca Raton, FL. 117–159.
22. Gingell, D., and L. Ginsberg. 1978. Problems in the physical interpretation of membrane interaction and fusion. *In* Membrane Fusion. G. Poste and G. L. Nicolson, editors. Elsevier/North Holland, Amsterdam. 791–833.
23. Knight, D. E., and M. C. Scrutton. 1986. Gaining access to the cytosol: the technique and some applications of electropermeabilization. *Biochem. J.* 234:497–506.
24. Neumann, E. 1984. Electric gene transfer into culture cells. *Bioelectrochem. Bioenerg.* 13:219–223.
25. Tsong, T. Y. 1983. Voltage modulation of membrane permeability and energy utilization in cells. *Biosci. Rep.* 3:487–505.
26. Sowers, A. E., and M. R. Lieber. 1986. Electropore diameters, lifetimes, numbers, and locations in individual erythrocyte ghosts. *FEBS (Fed. Eur. Biochem. Soc.) Lett.* 205:179–184.
27. Mehrle, W., U. Zimmermann, and R. Hamp. 1985. Evidence for

asymmetrical uptake of fluorescent dyes through electropermeabilized membranes of *Avena* mesophyll protoplasts. *FEBS (Fed. Eur. Biochem. Soc.) Lett.* 185:89–94.

28. Rossignol, D. P., G. L. Decker, W. J. Lennarz, T. Y. Tsong, and J. Teissie. 1983. Induction of calcium-dependent, localized cortical granule breakdown in sea-urchin eggs by voltage pulsation. *Biochim. Biophys. Acta.* 763:346–355.
29. Balasubraminian, A., and S. McLaughlin. 1982. Electro-osmosis at the surface of phospholipid bilayer membranes. *Biochim. Biophys. Acta.* 685:1–5.
30. Breckenridge, L. J., and W. Almers. 1987. Final steps in exocytosis observed in cells with giant secretory granules. *Proc. Natl. Acad. Sci. USA.* 84:1945–1949.
31. Fernandez, J. M., E. Neher, and B. D. Gomperts. 1984. Capacitance measurements reveal stepwise fusion events in degranulating mast cells. *Nature (Lond.)* 312:453–455.
32. Zimmerberg, J., M. Curran, F. S. Cohen, and M. Brodwick. 1987. Simultaneous electrical and optical measurements show that membrane fusion precedes secretory granule swelling during exocytosis of beige mouse mast cells. *Proc. Natl. Acad. Sci. USA.* 84:1585–1589.
33. Neumann, E., A. E. Sowers, and C. Jordan. 1988. Electroporation and Electrofusion in Cell Biology. Plenum Press, New York. In press.